Journal of Research in Pharmacy

Research Article

www.jrespharm.com

Antiviral Properties of 5-Sulfamoyl-1*H*-Indole-Linked Spirothiazolidinone Derivatives: A Study on Human Parainfluenza Virus-2

Muhammed TRAWALLY [1], Fatıma Nur YILMAZ [2], Berna ÖZBEK ÇELİK [2], Atilla AKDEMİR [3], Özlen GÜZEL AKDEMİR [1]*

1 Department of Pharmaceutical Chemistry, Faculty of Pharmacy, Istanbul University, Beyazit 34116, Fatih, Istanbul, Türkiye.
2 Department of Pharmaceutical Microbiology, Faculty of Pharmacy, Istanbul University, Beyazit 34116, Fatih, Istanbul, Türkiye.
3 Department of Pharmacology, Faculty of Pharmacy, Istinye University, Istanbul, Türkiye.
* Corresponding Author. E-mail: oguzel@istanbul.edu.tr (O.G.A).

Received: 25 November 2023 / Accepted: 27 December 2023

ABSTRACT: Human parainfluenza viruses (HPIVs) are responsible for a wide range of respiratory infections in humans, particularly in children, the elderly, and immunocompromised individuals. This paper presents a study regarding the antiviral activity of a series of 3-phenyl-5-sulfamoyl-*N*-(7/8/9-(non)substituted-3-oxo-1-thia-4-azaspiro[4.4]non/[4.5]dec-4-yl)-1*H*-indole-2-carboxamide derivatives against HPIV-2. Our findings suggest the compounds displayed low potency against HPIV-2. Compounds **4** and **8** exhibited the most potent antiviral effects with inhibition of 95.46 and 90.90 % at 10 mg/mL, respectively. Molecular modeling studies were conducted on hemagglutinin-neuraminidase, a crucial druggable target for HPIV, to predict the binding modes of the compounds.

KEYWORDS: parainfluenza virus; HPIV-2; indole; thiazolidinone; hemagglutinin-neuraminidase; molecular docking.

1. INTRODUCTION

HPIVs are a group of respiratory pathogens that cause various acute respiratory diseases, such as pneumonia, bronchitis, and bronchiolitis. These diseases stand as the primary cause of death among children aged below five years, contributing to approximately two to three million childhood deaths annually and approximately 20% of all childhood fatalities globally[1–4]. HPIVs are part of the *Paramyxoviridae* family and are classified into 4 types. Types 1 and 3 belong to the *Respirovirus* family, whereas types 2 and 4 belong to the *Rubulavirus* family [5]. HPIV type 2 (HPIV-2) is responsible for 60% of the HPIV-caused infections [6]. In conjunction with other viral agents such as the influenza virus, rhinovirus, and respiratory syncytial virus, HPIVs constitute a substantial proportion of respiratory viral infections that require medical intervention. These viruses are highly contagious, spread rapidly in crowded environments and primarily affect newborns, children, and those with weakened immune systems. Although vaccines and various antivirals are actively being studied in children and immunocompromised individuals, so far there are no specific antiviral therapies available for the treatment of HPIV infections except for symptomatic treatment with corticosteroids [7–9]. Although ribavirin has been considered a potential antiviral for HPIV based on laboratory studies, its efficacy has not been established. However, several cases of both positive and negative outcomes in nonrandomized studies have been reported. The use of ribavirin medication for the treatment of HPIV infection is not recommended due to the lack of evidence supporting its efficacy in improving clinical outcomes [10,11]. Therefore, there is a need for the development of new antiviral agents that can effectively treat these infections.

The mechanism by which HPIV penetrates the host cells starts by fusing its membrane with the cellular surface. The fusion process comprises the interaction between two vital proteins, hemagglutinin-neuraminidase (HN) and the fusion protein (F). HN facilitates the attachment of the HPIV to the host cell and activates the F protein that was initially hidden and inactive to undergo conformational changes and hence initiate the membrane fusion process. The activated F protein allows the union of the HPIV and the cellular

How to cite this article: Trawally M, Yılmaz FN, Özbek Çelik B, Akdemir A, Güzel Akdemir Ö. Antiviral Properties of 5-Sulfamoyl-1H-Indole-Linked Spirothiazolidinone Derivatives: A Study on Human Parainfluenza Virus-2. J Res Pharm. 2024; 28(1): 213-224.

ISSN: 2630-6344

http://dx.doi.org/10.29228/jrp.689

Journal of Research in Pharmacy
Research Article

membrane of the host, allowing the virus to penetrate the host cell [12,13]. Nevertheless, the premature activation of the F protein causes HPIV to lose its infectivity. Multiple studies have reported that certain antiviral agents exert their mechanism of action by promoting premature activation of the F protein, thus preventing the virulence of HPIV[14,15]. On the other hand, certain antiviral agents function by inhibiting the HN protein, hindering the fusion process of the HPIV virus to the host cells[7,12,13,15,16]. In addition, the HN protein has other activities including binding to sialic acid receptors, causing hemagglutination, and cleaving them through its neuraminidase activity. The HN protein is a complex structure with many components such as a cytoplasmic domain, a membrane-spanning region, a stalk region, and a globular head. The globular head region houses the major binding site for sialic acid and the enzymatic activity site for neuraminidase. The major binding site plays a crucial role in the initiation of fusion by HN [14,17].

Multiple heterocyclic compounds, including but not limited to indole and thiazolidinone, have been explored as promising candidates for the development of antiviral agents[18–23]. The indole is one of the "privileged scaffolds" found in many biologically active compounds used in the treatment of multiple diseases[24–27]. In addition, the indole skeleton is present in many agents that are commercially available or undergoing clinical trials (**Figure 1**)[28,29].

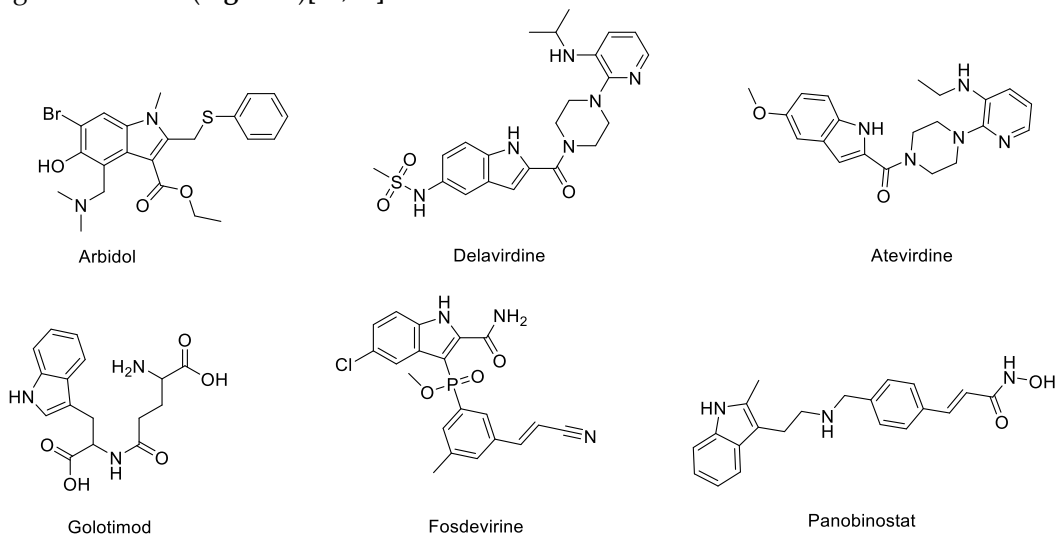

Figure 1. Antiviral compounds containing indole scaffold

On the other hand, spirothiazolidinones have various biological activities ranging from antibacterial, antimycobacterial [26,30], antiviral [31] and anticancer. Multiple studies have presented spirothiazolidinones as promising antiviral candidates, particularly against influenza A virus [31–36]. The incorporation of two or more promising bioactive scaffolds into a single molecule, resulting in the formation of hybrids, is a popular explored strategy within the field of drug discovery because hybrid molecules can often result in synergistic effects derived from each bioactive scaffold.

Previously, our team successfully synthesized and characterized a series of 3-phenyl-5-sulfamoyl-*N*-(7/8/9-(non)substituted-3-oxo-1-thia-4-azaspiro[4.4]non/[4.5]dec-4-yl)-1*H*-indole-2-carboxamide derivatives (compounds **1 – 18**), exhibiting potent antibacterial activity[26]. Encouraged by these findings and the above-mentioned antiviral properties of indole and spirothiazolidinone derivatives, we were inspired to explore the potential antiviral activity of compounds **1 – 18** against HPIV-2. Hence, this study presents the antiviral activity of these derivatives, and proposes the probable underlying mechanisms by which they exert their effects.

2. RESULTS AND DISCUSSION

2.1. Chemistry

The synthesis of 3-phenyl-5-sulfamoyl-*N*-(7/8/9-(non)substituted-3-oxo-1-thia-4-azaspiro[4.4]non/[4.5]dec-4-yl)-1*H*-indole-2-carboxamide derivatives (**1 – 18**) is a one-pot facile synthesis as illustrated in **Scheme 1** using 2-(hydrazinecarbonyl)-3-phenyl-1*H*-indole-5-sulfonamide as a starting material. The structures were confirmed with spectral analyses as reported by Güzel-Akdemir et al. [26].

http://dx.doi.org/10.29228/jrp.689
J Res Pharm 2024; 28(1): 213-224

Journal of Research in Pharmacy
Research Article

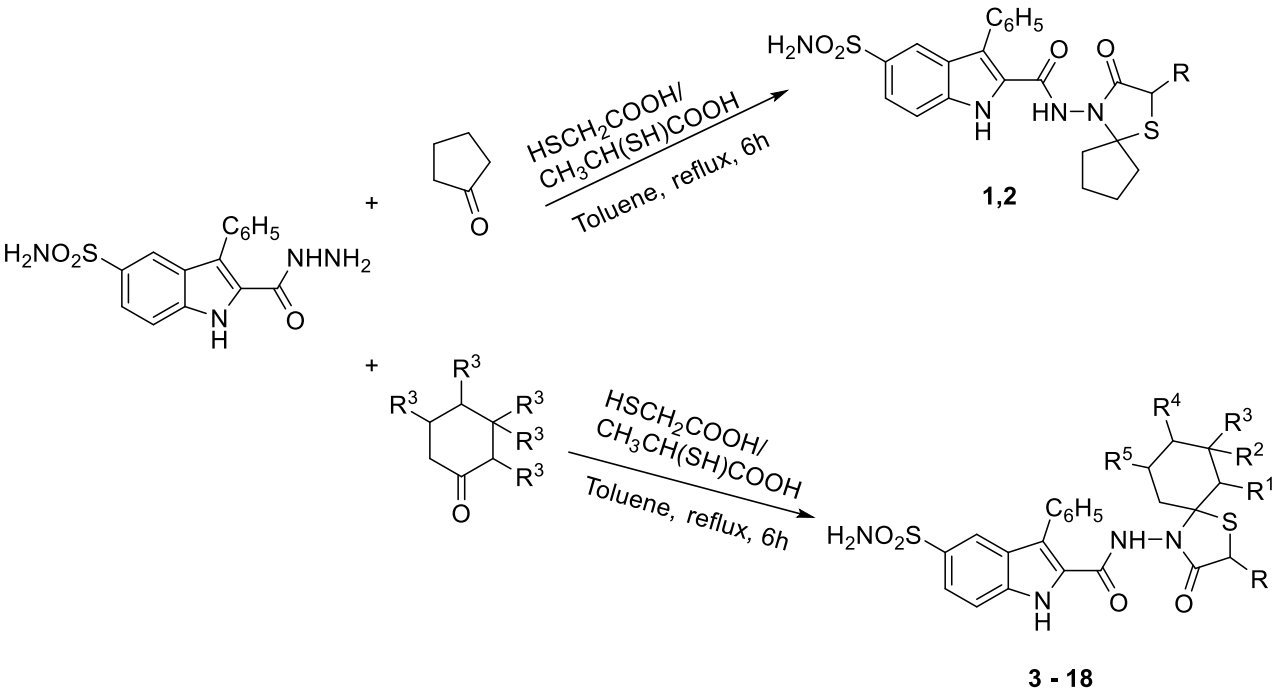

Scheme 1. Synthesis route of compounds 1 - 18

2.2. Antiviral Activity

The antiviral activity of compounds **1 – 18** against HPIV was evaluated using MTT cell viability assay (**Table 1**). At 10mg/ml, the compounds showed inhibition of HPIV with compound **4** displaying the highest inhibition of 95.46%. Analysis of the antiviral activity reveals that there is no direct structure-activity relationship (SAR). However, the increase in the size of the spiro ring in compound **1** to have compound **3**, improved the activity. Comparing compounds **1** and **2** containing the spiro-fused cyclopentane, the introduction of a methyl group to the thiazolidinone ring (compound **2**) enhanced the antiviral activity. On the contrary, in spiro-fused cyclohexanes, the introduction of a methyl group to the thiazolidinone (compound **11**) ring reduced the antiviral activity as observed in compounds **3** and **11**. However, the same trend is not observed in the rest of the non-methyl and methyl-substituted analogues. Nevertheless, in the non-methyl analogues of spiro-fused cyclohexanes (compounds **3 – 10**), the addition of a methyl group to the 7th position of the spirothiazolidinone yielded the most active compound, 4, against HPIV. However, two methyl groups decreased the activity. When compared to compound **3** (78.42%), the addition of aliphatic/aromatic groups to the 8th position decreased the activity except for compound **8** (90.9%) and **10** (86.01%) with a *tert*-butyl and phenyl groups, respectively, having an improved antiviral activity.

On the other hand, the addition of aliphatic/aromatic groups to the spirothiazolidinone ring of the methyl-substituted analogues of spiro-fused cyclohexanes (compounds **11 – 18**) improved the antiviral activity. However, increasing the size of the aliphatic chain on position 8 decreased the activity, while the presence of a phenyl ring (compound **18**) increased the activity. Furthermore, it is observed that the addition of a methyl group at position 7 favoured the activity better than the substitution at other positions (compound **13**).

http://dx.doi.org/10.29228/jrp.689
J Res Pharm 2024; 28(1): 213-224

Table 1. Antiviral activity of 3-phenyl-5-sulfamoyl-*N*-(7/8/9-(non) substituted-3-oxo-1-thia-4-azaspiro[4.4]non/[4.5]dec-4-yl)-1*H*-indole-2-carboxamide derivatives (**1 – 18**)

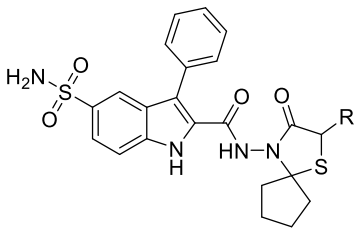

1,2

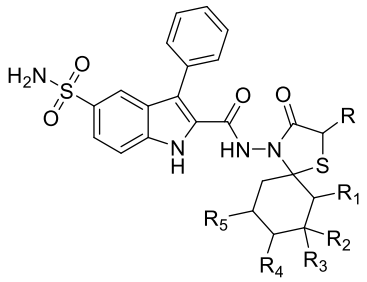

3 - 18

Compounds	R	R^1	R^2	R^3	R^4	R^5	10mg/ml
1	H	-	-	-	-	-	57.48
2	CH_3	-	-	-	-	-	76.82
3	H	H	H	H	H	H	78.42
4	H	H	CH_3	H	H	H	95.46
5	H	H	H	H	CH_3	H	66.56
6	H	H	H	H	C_2H_5	H	74.46
7	H	H	H	H	C_3H_7	H	51.16
8	H	H	H	H	*tert*-C_4H_9	H	90.90
9	H	H	CH_3	CH_3	H	CH_3	69.11
10	H	H	H	H	C_6H_5	H	86.01
11	CH_3	H	H	H	H	H	55.44
12	CH_3	CH_3	H	H	H	H	87.48
13	CH_3	H	CH_3	H	H	H	85.07
14	CH_3	H	H	H	CH_3	H	82.87
15	CH_3	H	H	H	C_2H_5	H	79.35
16	CH_3	H	H	H	C_3H_7	H	76.63
17	CH_3	H	H	H	*tert*-C_4H_9	H	76.50
18	CH_3	H	H	H	C_6H_5	H	84.50

2.3. *In Silico* Studies

2.3.1. ADME Prediction

15 parameters important for assessing the ADME and drug-likeness of the compounds were evaluated (**Table 2**). Among the compounds, only compounds **1 – 4** and **11** did not violate RO5 due to the lower (<500 g/mol) molecular weight of the compounds. Also, the compounds generally violated the aqueous solubility (QPlogS) except compounds **1 – 5** and **11.** All the compounds were shown to be CNS inactive due to their polarity hindering them from crossing the BBB. Besides, the QPlogBB which predicts the brain/blood partition coefficient is between -2.187 – -1.671, demonstrating a general BBB permeability. In addition, the compounds demonstrated medium cell permeability (QPPCaco). All the compounds are within the recommended values for binding to human serum albümin (logKhsa) and have a percentage human oral absorption of more than 65% with compound **4**-RS and SR displaying the highest absorption of 81.773 and 81.852%, respectively.

Table 2 ADME and drug-likeness properties of compounds **1 – 18**

Title	donor HB	Accpt HB	CNS –2 (inactive), +2 (active)	mol MW (130.0 – 725.0)	QPlogPo/w (–2.0 – 6.5)	QPlogS (–6.5 – 0.5)	QPPCaco (<25 poor, >500 great)	QPlogBB (–3.0 – 1.2)	QPlogKhsa (–1.5 – 1.5)	HOA (1=low, 2=medium, 3=high)	PHOA (>80% is high <25% is poor)	#metab (1 – 8)	PSA (7.0 – 200.0)	RO5	RO3
1	3.250	9.250	-2	470.560	2.427	-5.765	84.856	-1.892	0.212	3	75.676	1	142.138	0	1
2-S	3.250	9.250	-2	484.587	2.805	-6.211	105.570	-1.860	0.344	1	79.586	1	138.769	0	1
2-R	3.250	9.250	-2	484.587	2.801	-6.203	105.911	-1.856	0.341	1	79.591	1	140.182	0	1
3	3.250	9.250	-2	484.587	2.701	-6.049	87.570	-1.902	0.326	3	77.527	1	140.834	0	1
4-SS	3.250	9.250	-2	498.614	3.036	-6.456	91.695	-1.911	0.450	1	79.843	1	140.654	0	1
4-RS	3.250	9.250	-2	498.614	3.087	-6.094	113.058	-1.671	0.448	3	81.773	1	136.621	0	1
4-SR	3.250	9.250	-2	498.614	3.067	-6.121	115.946	-1.678	0.435	3	81.852	1	137.032	0	1
4-RR	3.250	9.250	-2	498.614	3.025	-6.533	87.376	-1.960	0.449	1	79.405	1	140.724	0	1
5	3.250	9.250	-2	498.614	3.024	-6.488	89.182	-1.937	0.447	1	79.557	1	140.672	0	1
6	3.250	9.250	-2	512.641	3.353	-6.811	87.726	-2.060	0.535	1	68.396	1	140.628	1	1
7	3.250	9.250	-2	526.667	3.711	-7.194	87.420	-2.187	0.634	1	70.464	1	140.831	1	1
8	3.250	9.250	-2	540.694	3.884	-7.351	87.886	-2.069	0.754	1	71.521	1	140.691	1	1
9-SR	3.250	9.250	-2	526.667	3.561	-7.066	88.414	-1.972	0.673	1	69.675	1	140.359	1	1
9-RR	3.250	9.250	-2	526.667	3.295	-6.313	65.078	-1.866	0.637	1	65.737	1	138.409	1	1
9-SS	3.250	9.250	-2	526.667	3.111	-5.734	76.910	-1.668	0.553	2	65.955	1	135.950	1	1
9-RS	3.250	9.250	-2	526.667	3.577	-7.014	90.969	-1.941	0.679	1	69.992	1	140.261	1	1
10	3.250	9.250	-2	560.685	4.279	-7.876	91.151	-2.057	0.862	1	74.117	3	141.353	1	1
11-R	3.250	9.250	-2	498.614	3.061	-6.406	113.365	-1.827	0.447	1	81.637	1	139.755	0	1
11-S	3.250	9.250	-2	498.614	3.063	-6.485	110.920	-1.861	0.448	1	81.482	1	139.657	0	1
12-RR	3.250	9.250	-2	512.641	3.359	-6.698	129.486	-1.783	0.553	1	71.460	1	135.793	1	1
12-SR	3.250	9.250	-2	512.641	3.319	-6.647	125.555	-1.788	0.540	1	70.987	1	135.817	1	1
12-RS	3.250	9.250	-2	512.641	3.386	-6.659	124.253	-1.774	0.570	1	71.298	1	136.881	1	1
12-SS	3.250	9.250	-2	512.641	3.349	-6.524	118.053	-1.760	0.564	1	70.681	1	137.784	1	1
13-RS	3.250	9.250	-2	512.641	3.355	-6.801	108.376	-1.872	0.564	1	70.055	1	138.556	1	1

How to cite this article: Trawally M, Yılmaz FN, Özbek Çelik B, Akdemir A, Güzel Akdemir Ö. Antiviral Properties of 5-Sulfamoyl-1H-Indole-Linked Spirothiazolidinone Derivatives: A Study on Human Parainfluenza Virus-2. J Res Pharm. 2024; 28(1): 213-224.

ISSN: 2630-6344
http://dx.doi.org/10.29228/jrp.689

13-SS	3.250	9.250	-2	512.641	3.400	-6.970	109.330	-1.917	0.581	1	70.383	1	138.611	1	1
13-RR	3.250	9.250	-2	512.641	3.363	-6.823	109.321	-1.874	0.565	1	70.166	1	138.736	1	1
13-SR	3.250	9.250	-2	512.641	3.400	-6.966	109.720	-1.914	0.581	1	70.415	1	138.805	1	1
14-R	3.250	9.250	-2	512.641	3.401	-6.970	108.562	-1.919	0.582	1	70.335	1	138.619	1	1
14-S	3.250	9.250	-2	512.641	3.359	-6.797	109.838	-1.864	0.564	1	70.182	1	138.607	1	1
15-R	3.250	9.250	-2	526.667	3.726	-7.270	108.514	-2.025	0.668	1	72.235	1	138.535	1	1
15-S	3.250	9.250	-2	526.667	3.687	-7.106	109.726	-1.973	0.651	1	72.095	1	138.593	1	1
16-R	3.250	9.250	-2	540.694	4.052	-7.498	109.973	-2.095	0.752	1	74.246	1	141.090	1	1
16-S	3.250	9.250	-2	540.694	4.083	-7.657	107.869	-2.151	0.768	1	74.276	1	138.824	1	1
17-R	3.250	9.250	-2	554.721	4.261	-7.817	109.160	-2.033	0.889	1	75.412	1	138.630	1	1
17-S	3.250	9.250	-2	554.721	4.218	-7.657	109.155	-1.989	0.871	1	75.161	1	138.616	1	1
18-R	3.250	9.250	-2	574.711	4.635	-8.378	108.085	-2.053	0.995	1	77.525	3	139.307	1	1
18-S	3.250	9.250	-2	574.711	4.596	-8.223	107.911	-2.011	0.977	1	77.285	3	138.667	1	1

Journal of Research in Pharmacy
Research Article

2.3.2. Molecular Docking

The crystal structure of hPIV-2 HN protein is not available and thus, hPIV-3 HN protein co-crystallized with zanamivir is utilized for the docking studies. Using the Basic Local Alignment Search Tool (BLAST), hPIV-2 HN and hPIV-3 HN showed 28% similarity with conserved amino acid residues like Arg192, Arg424, Arg502, Tyr530 that are crucial for the activity of sialidase. BLAST is a widely used bioinformatics program for quickly searching sequence databases and sequence similarity. It can conduct a sequence similarity search for a sequence of interest against a curated sequence database. BLAST can find query sequence homologs and detect statistically significant pairwise sequence alignments even at low sequence identity[37].

As observed in **Figure 2A**, Zanamivir formed six hydrogen bonds with Thr193, Glu276, Arg424, Arg502 and Tyr530, and a salt bridge with Glu409. To validate the applied docking protocol, a redocking of zanamivir was conducted and the obtained docked pose was very similar to the binding pose of the co-crystallized ligand with an RSMD value of 0.27 A (**Figure 2A).** Docking studies on the most active compounds among the spiro-fused cyclopentanes and cyclohexanes, compounds **2** and **4**, respectively, were conducted to rationalize the activity difference. The docked poses were analyzed based on the ligand low energy conformation, protein interactions and complementarity. Compound **2** has two enantiomers (R and S). Compound **2-R** showed a better-docked pose than SR with a docking score of -3.45 kcal/mol and formed hydrogen bonds with Ile 474 and Tyr530 and a π-π interaction with Arg424 (**Figure 2B**). Compound 4 has diastereomers (RR, SS, RS and SR). Compound **4-RR** showed the best favourable docked pose with a docking score of -4.42 kcal/mol and formed two hydrogen bonds with Ile474 and Tyr530 and a π-π interaction with Arg424. (**Figure 2C**). Comparing the docked poses of compounds **2-R** and **4-RR**, it is observed that the enlargement of the cycloalkane ring from cyclopentane to cyclohexane enhances hydrophobic interactions with Pro272 and Tyr319. This might explain the subtle difference between the antiviral activities of the two compounds. The binding poses of zanamivir (green), compound **2-R** (yellow) and compound **4-RR** (turquoise) were superposed in **Figure 2D**, showing that the compounds fit well in the binding pocket.

How to cite this article: Trawally M, Yılmaz FN, Özbek Çelik B, Akdemir A, Güzel Akdemir Ö. Antiviral Properties of 5-Sulfamoyl-1H-Indole-Linked Spirothiazolidinone Derivatives: A Study on Human Parainfluenza Virus-2. J Res Pharm. 2024; 28(1): 213-224.

http://dx.doi.org/10.29228/jrp.689
ISSN: 2630-6344

Journal of Research in Pharmacy
Research Article

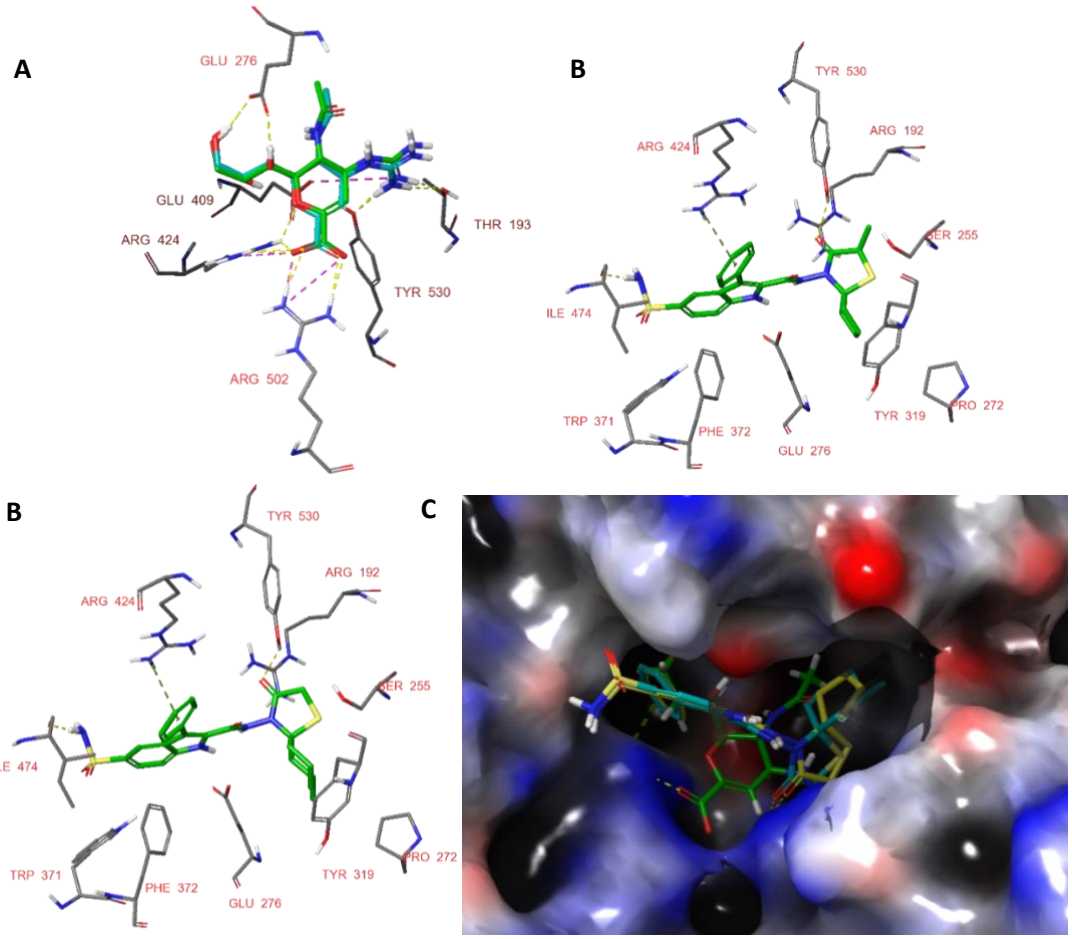

Figure 2. Docked poses of A) Zanamivir B) compound **2-R** C) compound **4-RR** Zanamivir (green), compound **2-R** (yellow) and compound **4-RR** (turquoise) in HPIV-2 HN (PDB: 1V3E)

3. CONCLUSION

This study evaluated the antiviral activities of spirothiazolidinone linked with 5-sulfamoyl-1*H*-indole derivatives (**1 – 18**) against HPIV-2. The findings indicate that these hybrid compounds exhibit antiviral activity against HPIV-2 at 10mg/mL. Notably, compound **4** demonstrated the highest antiviral efficacy with an inhibition of 95.46% at a concentration of 10 mg/mL. The observation of the antiviral activity of these compounds at such high concentrations indicates that these hybrids exhibit a low level of effectiveness against HPIV-2, and there is still significant potential for enhancement, necessitating further structural modification and optimization for better effectiveness.

4. MATERIALS AND METHODS

4.1. Chemistry

All the chemicals used for the synthesis and devices used for the characterization of the compounds were reported in our previously published work.

Synthesis of ***3-phenyl-5-sulfamoyl-N-(3-oxo-1-thia-4-azaspiro[4.4]non/[4.5]dec-4-yl)-1H-indole-2-carboxamide derivatives*** **(1 – 18)**

Thioglycolic acid/thiolactic acid (20 mmol) was introduced into a round bottom flask containing 1.65g of compound **a** (5 mmol) and a suitable cyclic ketone (5 mmol, 1 eq) in 20 ml anhydrous toluene. The reaction was refluxed for 5-6 hours with the assistance of a Dean-Stark water separator. To remove surplus toluene, the mixture was concentrated. Saturated $NaHCO_3$ was applied to the resulting residue until the emission of CO_2 ceased. Occasionally, the reaction mixture was refrigerated until it solidified after being allowed to stand overnight. Following an H_2O wash and air-drying, the impure solid was recrystallized from ethanol[26].

4.2. Antiviral Activity

VERO cells were prepared in a medium containing 10% FBS at a concentration of 1x105 cells per millilitre. From this suspension, 100 microliters were added to each well of a 96-well microplate. The microplates were incubated for 24 hours in an oven with 5% CO_2 at 37°C. After incubation, the medium in the wells was discarded and washed with PBS. Parainfluenza virus stock suspensions were taken from a -152 °C freezer and dilutions were prepared after thawing. The first column of the 96-well microplate was used as the cell control, and the second column as the virus control. From the second column to the last one, 7 columns in total, 100 microliters of the prepared virus suspension were added to each well. The prepared compound suspensions were added synchronously with the viruses to the columns of the plates, with 100 microliters added to each well in one column for each compound. Only a culture medium with 1% FBS was added to the cell control well. Following the addition of the virus to the virus control well, 100 microliters of 1% FBS culture medium were added. The microplates were incubated at 37°C in a 5% CO_2 incubator for 3 days. During the incubation period, the virus control wells were checked under a microscope and observed for CPE. At the end of the 3 days, when CPE reached 90%, the liquids in the wells were discarded. The steps for MTT were followed to observe the antiviral effect. MTT stock solution was prepared at 5mg/ml in PBS. From the stock solution, 10 microliters were added to each well, followed by 90 microliters of phenol red-free DMEM. The microplates were incubated in a 37°C 5% CO_2 environment for 3 hours. After incubation, the formed formazan crystals were dissolved by removing the liquids from the wells and adding 100 microliters of DMSO, then left on a shaker for 15 minutes for the dye to dissolve completely. The microplates were read at 570 nm with an ELISA Reader (EON-BioTek Instruments, Winooski, VT, USA). Average absorbance values were calculated, and the percentage protection of the individual concentrations of the substances against the virus was calculated [38].

Protection % = (A - B)/(C - B) x 100
A = Average absorbance for each concentration of the substance in 8 wells
B = Virus control absorbance (average absorbance value of 8 wells)
C = Cell control absorbance (average absorbance value of 8 wells)

4.3. *In Silico* Studies

All molecular modeling studies were performed using the software tools of the Schrödinger package (v2023-3; Schrödinger, Inc., New York).

4.3.1 Preparation of ligands

The three-dimensional (3D) structures of all the ligands were generated using the Builder and LigPrep module was used to prepare the ligands. The possible stereoisomers were considered when constructing the compounds. During the preparation of the ligands, no tautomer was generated, and the ligands were energy-minimized using the OPLS4 force field.

4.3.2. In Silico ADME Predictions

Using the prepared ligands, the ADME properties and drug-likeness were subsequently predicted with the QikProp module. The number of hydrogen bond donors (donorHB) and acceptors (accptHB), octanol/water partition coefficient (QPlogPo/w), solubility (QPlogS), Caco cell permeability (QPPCaco), brain/blood partition coefficient (QPlogBB), (percentage of) human oral absorption, binding of human serum albumin, Van der Waals surface area (PSA), number of violations of the Lipinski Rule of Five (RO5), and the number of violations of Jorgensen's rule of three (RO3) were studied. The RO5 is commonly used for the assessment of the oral bioavailability and drug-like properties of small compounds. For a molecule to exhibit drug-like properties and demonstrate oral activity, it is required to have a molecular weight below 500 Da, a maximum of 5 hydrogen bond donors (donorHBs), a maximum of 10 hydrogen bond acceptors (accptHBs), a logP value lower than 5, and it should not contravene more than one of these rules. The RO3 also evaluates the drug-like properties of lead compounds. According to the provided information, it is indicated that the minimum required value for QPlogS is -5.7, the minimum acceptable rate for QPPCaco is 22 nm/s, and the maximum allowable count for primary metabolites is 7.

4.3.3. Protein preparation and receptor grid generation structures

The crystal structure of hPIV-3 HN in complex with Zanamivir (PDB: 1V3E, 1.89 Å) was obtained due to sequence similarity. Chain A of the crystal structure and its corresponding co-crystallized ligand were retained, whereas chain B and its ligands were deleted. Using the Protein Preparation Wizard, hydrogen atoms

were added, N- and C-terminals were capped, missing side chains were added, and the system was energy minimized using the OPLS4 forcefield. Using the receptor Grid Generation module, a grid box was generated around the center of each co-crystallized ligand within the protein crystal structure to define the binding pocket. Ligands with lengths of ≤ 20 Å were allowed to dock. Conformational flexibility was allowed for hydroxyl groups of amino acid residues located within 5 Å of co-crystallized ligands and are not involved in the protein hydrogen bonding network [39].

4.3.4. Molecular docking

Docking studies were conducted using the Glide module with Extra Precision (XP) employing the default settings. The planarity of the conjugated π groups was improved, docking penalties based on the Epik state were implemented, and each ligand was docked 25 times to produce the 3 best poses [39].

4.3.5. MM-GBSA binding free energy calculation.

Rescoring with MM-GBSA binding energy calculations was performed on the obtained XP docked poses using the Prime/MM-GBSA module to predict the binding free energy of the ligands to the receptor. The binding energy is calculated using the following formulas:

$$\Delta G_{bind} = \Delta E_{MM} + \Delta G_{solv} + \Delta G_{SA}$$

ΔG_{solv} indicates the difference in GB_{SA} solvation energy between the protein-ligand complex and the unliganded protein and ligand. ΔE_{MM} represents the difference in minimized energies between the protein-ligand complex and the sum of energies from the unliganded protein and ligand. ΔG_{SA} represents the energy difference between the complex and the sum of the unliganded protein and ligand surface area energies [40].

Acknowledgements: This research was funded by Istanbul University Scientific Research Projects under project Number: T-15108.

Author contributions: Concept – M.T., A.A, Ö.G.A.; Design – M.T., A.A, Ö.G.A.; Supervision – A.A, Ö.G.A, BÖÇ.; Data Collection and/or Processing – M.T, F.N.Y.; Analysis and/or Interpretation – M.T., F.N.Y, A.A, Ö.G.A, BÖÇ.; Literature Search – M.T.; Writing – M.T., F.N.Y, A.A; Critical Reviews – A.A, Ö.G.A.

Conflict of interest statement: The authors declared no conflict of interest.

REFERENCES

[1] Nair H, Nokes DJ, Gessner BD, Dherani M, Madhi SA, Singleton RJ, O'Brien KL, Roca A, Wright PF, Bruce N, Chandran A, Theodoratou E, Sutanto A, Sedyaningsih ER, Ngama M, Munywoki PK, Kartasasmita C, Simões EAF, Rudan I, Weber MW, Campbell H. Global burden of acute lower respiratory infections due to respiratory syncytial virus in young children: a systematic review and meta-analysis. Lancet Lond Engl. 2010; 375: 1545–55. https://doi.org/10.1016/S0140-6736(10)60206-1

[2] DeGroote NP, Haynes AK, Taylor C, Killerby ME, Dahl RM, Mustaquim D, Gerber SI, Watson JT. Human parainfluenza virus circulation, United States, 2011-2019. J Clin Virol Off Publ Pan Am Soc Clin Virol. 2020; 124: 104261. https://doi.org/10.1016/j.jcv.2020.104261

[3] Wang X, Li Y, Deloria-Knoll M, Madhi SA, Cohen C, Arguelles VL, Basnet S, Bassat Q, Brooks WA, Echavarria M, Fasce RA, Gentile A, Goswami D, Homaira N, Howie SRC, Kotloff KL, Khuri-Bulos N, Krishnan A, Lucero MG, Lupisan S, Mathisen M, McLean KA, Mira-Iglesias A, Moraleda C, Okamoto M, Oshitani H, O'Brien KL, Owor BE, Rasmussen ZA, Rath BA, Salimi V, Sawatwong P, Scott JA, Simões EAF, Sotomayor V, Thea DM, Treurnicht FK, Yoshida LM, Zar HJ, Campbell H, Nair H. Global burden of acute lower respiratory infection associated with human parainfluenza virus in children younger than 5 years for 2018: a systematic review and meta-analysis. Lancet Glob Health. 2021; 9: e1077–87. https://doi.org/10.1016/S2214-109X(21)00218-7

[4] Bhasin S, Nadar M, Hasija Y. Epicatechin analogues may hinder human parainfluenza virus infection by inhibition of hemagglutinin-neuraminidase protein and prevention of cellular entry. J Mol Model. 2022; 28: 319. https://doi.org/10.1007/s00894-022-05310-9

[5] Alsaleh AN, Aziz IM, Alkubaisi NA, Almajhdi FN. Genetic analysis of human parainfluenza type 2 virus in Riyadh, Saudi Arabia. Virus Genes. 2023: 1–8. https://doi.org/10.1007/s11262-023-02035-6.

[6] Lee K, Lee J, Perry K. Abstract 1256: The surface-specific antigenic peptide designs of HPIV-type 2 hemagglutinin-neuraminidase and fusion protein for anti-viral immunotherapy drug development. J Biol Chem. 2023; 299: 103991. https://doi.org/10.1016/j.jbc.2023.103991

[7] Bailly B, Dirr L, El-Deeb IM, Altmeyer R, Guillon P, von Itzstein M. A dual drug regimen synergistically blocks human parainfluenza virus infection. Sci Rep. 2016; 6: 24138. https://doi.org/10.1038/srep24138
[8] Rota P, La Rocca P, Bonfante F, Pagliari M, Piccoli M, Cirillo F, Ghiroldi A, Franco V, Pappone C, Allevi P, Anastasia L. Design, synthesis, and antiviral evaluation of sialic acid derivatives as ınhibitors of Newcastle Disease Virus hemagglutinin-neuraminidase: A translational study on Human Parainfluenza Viruses. ACS Infect Dis. 2023; 9: 617–630. https://doi.org/10.1021/acsinfecdis.2c00576
[9] Chibanga VP, Dirr L, Guillon P, El-Deeb IM, Bailly B, Thomson RJ, von Itzstein M. New antiviral approaches for human parainfluenza: Inhibiting the haemagglutinin-neuraminidase. Antiviral Res. 2019; 167: 89–97. https://doi.org/10.1016/j.antiviral.2019.04.001
[10] Smielewska A, Emmott E, Goodfellow I, Jalal H. In vitro sensitivity of human parainfluenza 3 clinical isolates to ribavirin, favipiravir and zanamivir. J Clin Virol Off Publ Pan Am Soc Clin Virol. 2018; 102: 19–26. https://doi.org/10.1016/j.jcv.2018.02.009
[11] Marcink TC, Englund JA, Moscona A. Paramyxoviruses: Parainfluenza Viruses. Viral Infect. Hum., Springer, New York, NY; 2022, p. 1–50. https://doi.org/10.1007/978-1-4939-9544-8_25-1
[12] Marcink TC, Yariv E, Rybkina K, Más V, Bovier FT, des Georges A, Greninger AL, Alabi CA, Porotto M, Ben-Tal N, Moscona A. Hijacking the fusion complex of human parainfluenza virus as an antiviral strategy. mBio. 2020; 11. https://doi.org/10.1128/mBio.03203-19
[13] Marcink TC, Wang T, Des Georges A, Porotto M, Moscona A. Human parainfluenza virus fusion complex glycoproteins imaged in action on authentic viral surfaces. PLoS Pathog. 2020; 16: e1008883. https://doi.org/10.1371/journal.ppat.1008883
[14] Farzan SF, Palermo LM, Yokoyama CC, Orefice G, Fornabaio M, Sarkar A, Kellogg GE, Greengard O, Porotto M, Moscona A. Premature activation of the paramyxovirus fusion protein before target cell attachment with corruption of the viral fusion machinery. J Biol Chem. 2011; 286: 37945–37954. https://doi.org/10.1074/jbc.M111.256248
[15] Guillon P, Dirr L, El-Deeb IM, Winger M, Bailly B, Haselhorst T, Dyason JC, von Itzstein M. Structure-guided discovery of potent and dual-acting human parainfluenza virus haemagglutinin-neuraminidase inhibitors. Nat Commun. 2014; 5: 5268. https://doi.org/10.1038/ncomms6268
[16] Eveno T, Dirr L, El-Deeb IM, Guillon P, von Itzstein M. Targeting Human Parainfluenza Virus Type-1 haemagglutinin-neuraminidase with mechanism-based ınhibitors. Viruses 2019; 11(5):417. https://doi.org/10.3390/v11050417
[17] Porotto M, Fornabaio M, Kellogg GE, Moscona A. A second receptor binding site on human parainfluenza virus type 3 hemagglutinin-neuraminidase contributes to activation of the fusion mechanism. J Virol. 2007; 81: 3216–3228. https://doi.org/10.1128/JVI.02617-06
[18] Barreca ML, Chimirri A, De Luca L, Monforte AM, Monforte P, Rao A, Zappalà M, Balzarini J, De Clercq E, Pannecouque C, Witvrouw M. Discovery of 2,3-diaryl-1,3-thiazolidin-4-ones as potent anti-HIV-1 agents. Bioorg Med Chem Lett. 2001; 11: 1793–1796. https://doi.org/10.1016/S0960-894X(01)00304-3
[19] Küçükgüzel G, Kocatepe A, de Clercq E, Sahin F, Güllüce M. Synthesis and biological activity of 4-thiazolidinones, thiosemicarbazides derived from diflunisal hydrazide. Eur J Med Chem. 2006; 41: 353–359. https://doi.org/10.1016/j.ejmech.2005.11.005
[20] Balzarini J, Orzeszko B, Maurin JK, Orzeszko A. Synthesis and anti-HIV studies of 2-adamantyl-substituted thiazolidin-4-ones. Eur J Med Chem. 2007; 42: 993–1003. https://doi.org/10.1016/j.ejmech.2007.01.003
[21] Cihan-Üstündağ G, Gürsoy E, Naesens L, Ulusoy-Güzeldemirci N, Çapan G. Synthesis and antiviral properties of novel indole-based thiosemicarbazides and 4-thiazolidinones. Bioorg Med Chem. 2016; 24: 240–246. https://doi.org/10.1016/j.bmc.2015.12.008
[22] Zhang GN, Li Q, Zhao J, Zhang X, Xu Z, Wang Y, Fu Y, Shan Q, Zheng Y, Wang J, Zhu M, Li Z, Cen S, He J, Wang Y. Design and synthesis of 2-((1H-indol-3-yl)thio)-N-phenyl-acetamides as novel dual inhibitors of respiratory syncytial virus and influenza virus A. Eur J Med Chem. 2020;186:111861. https://doi.org/10.1016/j.ejmech.2019.111861
[23] Dhadda S, Sharma S, Jakhar P, Sharma H. Contemporary progress in the green synthesis of spiro-thiazolidines and their medicinal significance: a review. RSC Adv. 2023; 13: 3723–3742. https://doi.org/10.1039/d2ra07474e
[24] Demir-Yazıcı K, Bua S, Akgüneş NM, Akdemir A, Supuran CT, Güzel-Akdemir Ö. Indole-based hydrazones containing a sulfonamide moiety as selective ınhibitors of tumor-associated human carbonic anhydrase ısoforms IX and XII. Int J Mol Sci. 2019; 20(9):2354. https://doi.org/10.3390/ijms20092354.
[25] Garg V, Maurya RK, Thanikachalam PV, Bansal G, Monga V. An insight into the medicinal perspective of synthetic analogs of indole: A review. Eur J Med Chem. 2019; 180: 562–612. https://doi.org/10.1016/j.ejmech.2019.07.019
[26] Güzel-Akdemir Ö, Trawally M, Özbek-Babuç M, Özbek-Çelik B, Ermut G, Özdemir H. Synthesis and antibacterial activity of new hybrid derivatives of 5-sulfamoyl-1H-indole and 4-thiazolidinone groups. Monatshefte Für Chem - Chem Mon. 2020; 151: 1443–1452. https://doi.org/10.1007/s00706-020-02664-9
[27] Güzel-Akdemir Ö, Demir-Yazıcı K, Vullo D, Supuran C, Akdemir A. New Pyridinium salt derivatives of 2-(Hydrazinocarbonyl)-3-phenyl-1H-indole-5-sulfonamide as selective ınhibitors of tumour-related human carbonic anhydrase ısoforms IX and XII. Anticancer Agents Med Chem. 2022; 22(14):2637-2646. https://doi.org/10.2174/1871520622666220207092123
[28] Zhang M-Z, Chen Q, Yang G-F. A review on recent developments of indole-containing antiviral agents. Eur J Med Chem. 2015; 89: 421–441. https://doi.org/10.1016/j.ejmech.2014.10.065.

[29] Dorababu A. Indole - a promising pharmacophore in recent antiviral drug discovery. RSC Med Chem. 2020; 11: 1335–1353. https://doi.org/10.1039/D0MD00288G

[30] Trawally M, Demir-Yazıcı K, Dingiş Birgül SI, Kaya K, Akdemir A, Güzel Ö. Mandelic acid-based spirothiazolidinones targeting M. tuberculosis: Synthesis, in vitro and in silico investigations. Bioorganic Chem. 2022; 121:105688. https://doi.org/10.1016/j.bioorg.2022.105688

[31] Vanderlinden E, Göktas F, Cesur Z, Froeyen M, Reed ML, Russell CJ, Cesur N, Naesens L. Novel inhibitors of influenza virus fusion: structure-activity relationship and interaction with the viral hemagglutinin. J Virol. 2010; 84: 4277–4288. https://doi.org/10.1128/JVI.02325-09

[32] Göktaş F, Vanderlinden E, Naesens L, Cesur N, Cesur Z. Microwave assisted synthesis and anti-influenza virus activity of 1-adamantyl substituted N-(1-thia-4-azaspiro[4.5]decan-4-yl)carboxamide derivatives. Bioorg Med Chem. 2012; 20: 7155–7159. https://doi.org/10.1016/j.bmc.2012.09.064

[33] Göktaş F, Vanderlinden E, Naesens L, Cesur Z, Cesur N, Taş P. Synthesis and structure-activity relationship of n-(3-oxo-1-thia-4-azaspiro[4.5]decan-4-yl)carboxamide ınhibitors of ınfluenza virus hemagglutinin mediated fusion. Phosphorus Sulfur Silicon Relat Elem. 2015; 190: 1075–1087. https://doi.org/10.1080/10426507.2014.965819

[34] Cihan-Üstündağ G, Naesens L, Şatana D, Erköse-Genç G, Mataracı-Kara E, Çapan G. Design, synthesis, antitubercular and antiviral properties of new spirocyclic indole derivatives. Monatshefte Für Chem - Chem Mon. 2019; 150: 1533–1544. https://doi.org/10.1007/s00706-019-02457-9

[35] Apaydın ÇB, Tansuyu M, Cesur Z, Naesens L, Göktaş F. Design, synthesis and anti-influenza virus activity of furan-substituted spirothiazolidinones. Bioorg Chem. 2021; 112: 104958. https://doi.org/10.1016/j.bioorg.2021.104958

[36] Soylu-Eter Ö, Duran GN, Özbil M, Göktaş F, Cihan-Üstündağ G, Karalı N. Antiviral activity and molecular modeling studies on 1H-indole-2,3-diones carrying a naphthalene moiety. J Mol Struct. 2023; 1281: 135100. https://doi.org/10.1016/j.molstruc.2023.135100

[37] Altschul SF, Madden TL, Schäffer AA, Zhang J, Zhang Z, Miller W, Lipman DJ. Gapped BLAST and PSI-BLAST: a new generation of protein database search programs. Nucleic Acids Res. 1997; 25: 3389–3402. https://doi.org/10.1093/nar/25.17.3389

[38] Chiang LC, Chiang W, Chang MY, Ng LT, Lin CC. Antiviral activity of *Plantago major* extracts and related compounds in vitro. Antiviral Res. 2002; 55: 53–62. https://doi.org/10.1016/s0166-3542(02)00007-4

[39] Trawally M, Demir-Yazıcı K, Dingiş-Birgül SI, Kaya K, Akdemir A, Güzel-Akdemir Ö. Dithiocarbamates and dithiocarbonates containing 6-nitrosaccharin scaffold: Synthesis, antimycobacterial activity and in silico target prediction using ensemble docking-based reverse virtual screening. J Mol Struct. 2023; 1277: 134818. https://doi.org/10.1016/j.molstruc.2022.134818

[40] Pattar SV, Adhoni SA, Kamanavalli CM, Kumbar SS. In silico molecular docking studies and MM/GBSA analysis of coumarin-carbonodithioate hybrid derivatives divulge the anticancer potential against breast cancer. Beni-Suef Univ J Basic Appl Sci. 2020; 9:36. https://doi.org/10.1186/s43088-020-00059-7